1-1-2010

Automatic classification of GPR signals

W Shao
University of Wollongong, wenbin@uow.edu.au

A Bouzerdoum
University of Wollongong, bouzer@uow.edu.au

S L. Phung
University of Wollongong, phung@uow.edu.au

L Su
University of Wollongong, lijun@uow.edu.au

B Indraratna
University of Wollongong, indra@uow.edu.au

See next page for additional authors

Automatic classification of GPR signals

Abstract

Ground penetrating radar has been widely used in many areas. However, the processing and interpretation of acquired signals remains a challenging task since it requires experienced users to manage the whole operations. In this paper, we propose an automatic classification system to categorise GPR signals based on magnitude spectrum amplitudes and support vector machines. The system is tested on a real-world GPR data set. The experimental results show that our system can correctly distinguish ground penetrating radar signals reflected by different materials.

Keywords

automatic, gpr, classification, signals

Disciplines

Physical Sciences and Mathematics

Publication Details

Shao, W., Bouzerdoum, A., Phung, S. L., Su, L., Indraratna, B. & Rujikiatkamjorn, C. (2010). Automatic classification of GPR signals. 2010 13th International Conference on Ground Penetrating Radar (GPR) (pp. 1-6). USA: IEEE.

Authors

W Shao, A Bouzerdoum, S L. Phung, L Su, B Indraratna, and C Rujikiatkamjorn

Automatic classification of GPR signals

W. Shao, A. Bouzerdoum, S. L. Phung
School of Electrical, Computer
and Telecommunications Engineering
University of Wollongong, Australia
Email: {ws909, bouzer, phung}@uow.edu.au

L. Su, B. Indraratna, C. Rujikiatkamjorn
School of Civil, Mining
and Environmental Engineering
University of Wollongong, Australia
Email: {lijun,indra,cholacha}@uow.edu.au

***Abstract*—Ground penetrating radar has been widely used in many areas. However, the processing and interpretation of acquired signals remains a challenging task since it requires experienced users to manage the whole operations. In this paper, we propose an automatic classification system to categorise GPR signals based on magnitude spectrum amplitudes and support vector machines. The system is tested on a real-world GPR data set. The experimental results show that our system can correctly distinguish ground penetrating radar signals reflected by different materials.**

Keywords-GPR, classification, magnitude spectrum, SVM

I. Introduction

Ground penetrating radar (GPR), sometimes called subsurface radar or ground probing radar, excels in non-destructive detection of objects that are beneath the shallow earth surface or in visually impenetrable structures, such as walls and concrete floors [1, 2, 3]. It has attracted considerable interest in many areas, such as archaeology, road construction, glacier and ice sheet investigation, and mineral exploration and resource evaluation.

Ground penetrating radar uses electromagnetic fields to detect subsurface objects. An electromagnetic wave propagating in the ground is partially reflected when hitting an object whose electromagnetic properties are different from surrounding materials. By analysing electromagnetic characteristics of the reflected wave, it is possible to identify the objects.

In this paper, we propose an automatic classification system based on magnitude spectrum amplitude features and support vector machines (SVMs). The proposed system can automatically select and extract features from a training data set, which minimises the subjectivity of a human operator.

This document is organized as follows. In Section II, we introduce the background of GPR processing techniques and support vector machines. In Section III the proposed automatic classification system is explained in detail. Then in Section IV we demonstrate the experimental data, procedures and results. Finally in Section V, concluding remarks are presented.

II. Review on GPR signal analysis

With GPR data processing, the general objective is to enhance the 2D time-distance record so that it can be interpreted by the human operator [2]. The initial step of GPR processing is 'dewow'. Dewow removes low-frequency components from the raw data and reduces the mean of each trace to a near zero level [2, 4, 5, 6]. These low-frequency components are usually noise caused by inductive effects or system dynamic range limitations.

The next step is to choose a time varying gain for the raw GPR data. Time varying gain is applied to compensate for the attenuation due to medium absorption, signal dispersion and spherical divergence [2, 7]. Then the next stage mostly involves filtering. Filtering is to improve the signal to clutter ratio and visual quality of the radar data [2, 4, 6]. There are two basic types of filtering: temporal filtering and spatial filtering. The temporal filtering is operated on the 1D trace, such as simple mean, low-pass filter and high-pass filters. The spatial filtering is performed across a number of traces, such as simple running average, average subtraction, spatial low-pass and high-pass filters.

Besides filtering, there are other techniques also available, such as de-convolution and migration. De-convolution tends to remove the source wavelet effect but seldom is of benefit for GPR processing [4, 5]. Migration addresses on directionality of the reflection data. Subject to antenna characteristics and electrical properties of the ground, the reflected electromagnetic waves are usually geometrically and spatially distorted. Migration is applied to correct this effect [4, 6, 8]. However, migration process requires a good understanding of subsurface wave velocity and is not good with complex and heterogeneous fields.

In addition, frequency analysis techniques have been used to aid GPR processing. Because GPR signal is non-stationary and time varying signal, approaches that provide information on both time and frequency contents of the signals are more suitable, compared to traditional methods such as Fourier transforms [9]. Time-frequency techniques have been widely used in radar and sonar signal processing [9, 10]. After processing, the data is usually visually interpreted by a human operator by identifying reflections or calculating depth. The interpretation can be performed either in 2D time-distance record or 3D GPR display. Additional tools, such as pattern recognition, trace attribute analysis and numerical modelling, may be used.

Al-Qadi et al. [11] proposed a time-frequency approach to evaluate GPR data for railway ballast assessment. Their approach utilises short-time Fourier transform (STFT). First, basic processing techniques such as vertical temporal and horizontal spatial filters are applied to remove low-frequency components from the data. Then STFT is applied to each trace. The

window length of the STFT is selected according to frequency resolution and time resolution. Finally, the energy attenuation of STFT results are used to assess ballast conditions. Shihab et al. [12] also utilize time-frequency characteristics to detect ballast deterioration. Their approach involves centre frequency analysis after STFT. In [12], a similar approach is deployed to detect ballast deterioration; it involves centre frequency analysis after short time Fourier transform.

Sinha et al. [13] presented a new method for time-frequency map computation for non-stationary signals. Traditional STFT has a limit on time-frequency resolution because the window length is pre-defined. This problem can be overcome by employing the continuous wavelet transform (CWT). Their experiments on seismic data show that, compared to STFT, the CWT approach has the advantage to detect frequency shadows and subtle stratigraphic features.

Fujimoto and Nonami [14] suggested a mine detection algorithm based on statistical features. To extract the features, firstly, they identify a frequency band where major differences between each frequency spectrum occur, and then select feature points within this frequency range. For each feature point, sample mean and sample variance of power spectra are calculated. Thereafter, population distribution can be evaluated using Student's *t*-distribution and chi-square distribution. By comparing the feature point distribution, it is possible to detect mines. Fujimoto and Nonami's experiments employ a sensor that combines GPR and a metal detector. They show that, compared to detection using a metal detector, their algorithm improves the probability of detection and decreases the probability of false alarm.

III. Proposed Method

In a GPR survey, reflected waves from different buried objects or paths present different electromagnetic characteristics, because particular resonance frequencies arise in wave propagation. Hence it is possible to classify the buried objects or underground material by analysing frequency spectra of received GPR signals. In the proposed system, features are extracted automatically and fed into a classification system. A system block diagram is shown in Fig. 1.

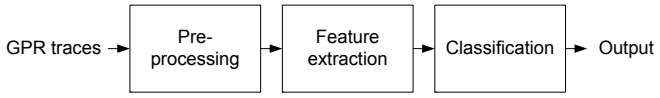

Fig. 1: Block diagram of the proposed automatic classification system.

A. Feature extraction

Let $s[n]$ be a GPR trace sequence of length L, $s[n] = 0$ for $n \geq L$. A discrete Fourier transform of $s[n]$ at the N equally spaced frequencies over $[0 \;\; 2\pi f_s)$ is mathematically expressed as

$$S[k] = \sum_{n=0}^{N-1} s[n] e^{-j2\pi \frac{k}{N} n}, \quad k = 0, 1, 2, \cdots, N-1 \qquad (1)$$

where f_s is the sampling frequency.

Additionally, the magnitude spectrum amplitudes are normalised as follows

$$P[k] = \frac{|S[k]|}{\sum_{k=0}^{N-1} |S[k]|} \qquad (2)$$

Figure 2 shows the magnitude spectra of six different traces whose antenna frequency is 800 MHz. It is observed that the majority of magnitude spectra has a frequency smaller than $2500MHz$, which is approximately three times as large as the GPR antenna frequency. Consequently unique features for each trace can be derived from this frequency range. In the proposed system, we choose the peak points of local maximum within the specific frequency range, and derive the amplitudes at these points. Then the amplitude values are arranged in the order of peak points for each trace, and fed into a classification system. Note that all the processing steps are done automatically by our system.

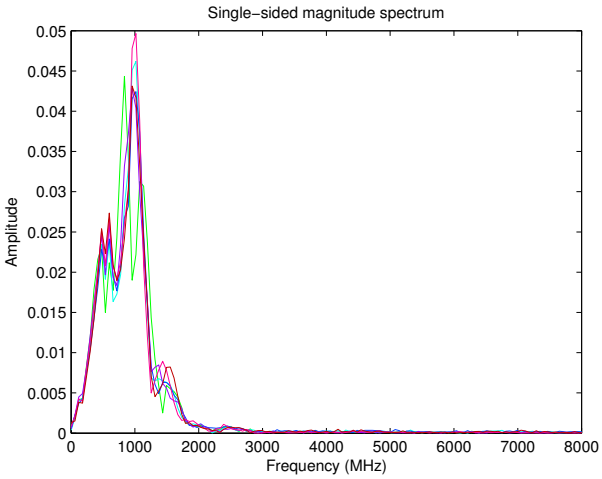

Fig. 2: Magnitude spectra of six different traces.

B. Classification

Support vector machines are originally formulated for two-class classification problems. In SVMs, the decision boundary is obtained from the training data by finding a separating hyperplane that maximizes the margins between the two classes; this is essentially a quadratic optimization problem. This learning strategy is shown to increase the generalization capability of the classifier. We can apply SVMs to complex non-linear problems by projecting the data onto a high-dimensional space and using kernel methods.

Suppose we have L training samples, each sample is in an $n-$dimensional space

$$\{(\mathbf{x}_1, y_1), (\mathbf{x}_2, y_2), \ldots, (\mathbf{x}_L, y_L)\},$$

where y_i is the class label, $y_i \in \{1, -1\}$. If the data are linearly separable in the input space, the decision function

can be written as

$$f(\mathbf{x}) = \langle \mathbf{w} \cdot \mathbf{x} \rangle + b \\ = \mathbf{w}^T \mathbf{x} + b \tag{3}$$

where $\mathbf{w}$ is an n-dimensional column vector, and b is a bias term, and $\langle \mathbf{w} \cdot \mathbf{x} \rangle$ is the dot product between $\mathbf{w}$ and $\mathbf{x}$.

There are many linear hyperplanes that can separate the data (Fig. 3a). However, only one hyperplane, called *optimal separating hyperplane*, can achieve maximum margin.

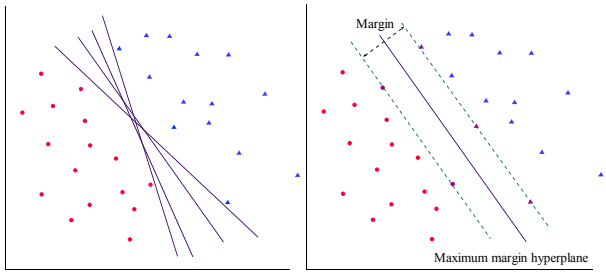

(a) Hyperplanes (b) Optimal hyperplane

Fig. 3: SVM optimal hyperplane for a two-class problem. (a) The data can be separated by many linear hyperplanes. (b) Only one hyperplane achieves maximum separation.

Provided the probability distribution of unknown data obeys the same law as that of training data, the optimal separating hyperplane classifies the data with maximized generalization ability [15, 16]. Therefore, the classification problem is to find proper $\mathbf{w}$ and b to maximize the margin of the training data. A constrained quadratic programming problem can be constructed to solve the problem. The objective is to minimize

$$Q(\mathbf{w}, b, \epsilon) = \frac{1}{2}\mathbf{w}^T\mathbf{w} + C \cdot \sum_{i=1}^{L} \epsilon_i \tag{4}$$

subject to the constraints

$$(\mathbf{w}^T\mathbf{x}_i + b) \cdot y_i \geq 1 - \epsilon_i \text{ and } \epsilon_i \geq 0 \text{ for } i = 1, 2, \ldots, L$$

where $\mathbf{w}$ is a vector perpendicular to the optimal separating hyperplane, b is a bias term, ϵ_i is a non-negative slack variable and C is the learning cost. The learning cost represents a compromise between margin maximization and classification error minimization.

Data of real-world applications are usually not linearly separable in the input space and the classifiers obtained in the original input space may not have high generalization ability for unknown data. By projecting data from the *input space* to a higher-dimensional *feature space* via a mapping function, it is possible to find a non-linear decision boundary for non-linear data in the input space. However, the projection is usually computation intensive. A kernel approach is proposed to simplify the projection. Among several proposed kernels, the RBF kernel has been demonstrated to yield good classification performance in diverse applications [17]. In this paper, we will focus on support vector machines with RBF kernel.

To solve a k-class problem, we construct $k(k-1)/2$ two-class SVM classifiers and each SVM classifier is trained with samples from two classes. This strategy is called *pair-wise support vector machines*.

IV. Results and Analysis

To evaluate the performance, the proposed system is applied to classify ballast conditions using a real-world GPR data set. The real-world data set is a part of a project on railway ballast evaluation using GPR, and it is obtained at Wollongong station in New South Wales, Australia.

Being a cost-effective and environment-friendly means of transportation, railway plays an important role in daily life. To ensure the safety, regular inspection of rail tracks must be conducted. The traditional rail examination method is usually labour intensive. In recent years, as a non-destructive detection tool, ground penetrating radar has been applied to railway ballast assessment to reduce labour and the cost. A challenging task arising is how to interpret the GPR signals and determine the ballast deterioration.

In this section, first we describe the data set, then data processing within the proposed system is explained. In the following section, how to extract feature vectors is given through an example. Finally, we present and analyse the experimental results.

A. Railway GPR data set

A railway track structure typically consists of rail, fastening system, sleepers, ballast, subballast and subgrade. A transverse section of typical railways is given in Fig. 4. The ballast is an essential component for proper railway functioning. To evaluate ballast deterioration using ground penetrating radar, three sections filled with different ballast are built into the existing railway. Each of them has a length of 200 cm and a depth of 55 cm (see Fig. 5). Based on the ballast conditions, the three sections are: (i) ballast mixed with 50% clay, (ii) clean ballast, and (iii) ballast mixed with 50% coal.

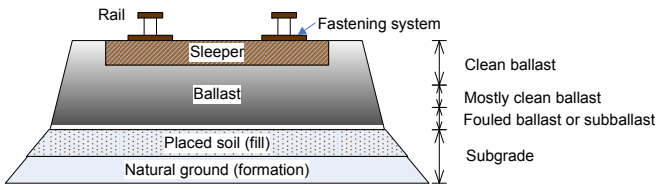

Fig. 4: Rail track structure, adopted from [11].

Two antennas of central frequencies 800 MHz and 1.2 GHz have been deployed in the surveys. There are 24 GPR profiles for 800 MHz and 12 profiles for 1.2 GHz. A summery of the radar profiles is given in Table I. For each radar profile, the GPR scans a whole section and different GPR configuration parameters, including antenna height, time window and sampling frequency, have been used. In the surveys, two antenna heights 20 cm and 30 cm have been applied. The antenna elevations can prevent the ground penetrating radar from collisions with varieties of devices along the railway.

To eliminate the border effects, the first 15% and last 15% traces of each GPR profile are discarded. Therefore, with $800\ MHz$ antenna, we have 981 traces for $20\ cm$ antenna height, and 984 traces for $30\ cm$ antenna height; with $1.2\ GHz$ antenna, there are 736 traces and 249 traces for $20\ cm$ antenna height and $30\ cm$ antenna height, respectively. The number of traces available for each section is shown in Table II.

B. Data processing

A problem of traditional GPR data processing techniques is that users subjectivity may be introduced. Therefore, in the pre-processing phase of our system only DC offset is applied to each trace to have zero mean. This minimizes the influence of a human operator and can be done automatically.

Next, every GPR trace is re-sampled to ensure all data is sampled using the same sampling frequency. In addition, each trace is shifted according to the position of the global maximum point. This shifting lowers the effects brought by different antenna heights. At the end of this stage, discrete Fourier transform is applied to obtain amplitude spectra. Afterwards, a number of random traces are selected to choose the proper feature points in the frequency range $(0,\ 3f)$, where f is the GPR antenna frequency. Then magnitude spectrum amplitude features are extracted at these feature points. It should be noted that the size of feature vector may vary when different data sets are used, because feature point selection depends on the randomly selected traces.

Finally, the feature vectors are fed into the classification stage. The feature data set is first divided into training set and test set. Then the training set is used to train the classifier, and test set is used to obtain the performance of the classifier. Our system uses pair-wise support vector machines with RBF kernel to perform classification. To train and evaluate the SVM classifiers, we used the SVM library *LIBSVM* [18], developed by Chang et al. at National Taiwan University. Five-fold cross validation on a grid search is applied to perform parameter selection of the SVMs.

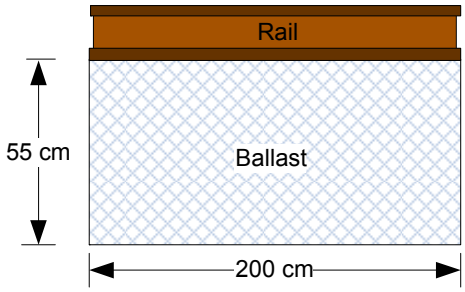

Fig. 5: Ground truth of the experimental fields.

TABLE I: A summary of GPR profiles of the railway data set. Section 1 is ballast mixed with 50% clay, Section 2 is clean ballast and Section 3 is ballast mixed with 50% coal.

GPR profiles				
Antenna frequency	$800\ MHz$		$1.2\ GHz$	
Antenna height	$20cm$	$30cm$	$20cm$	$30cm$
Section 1	4	4	3	3
Section 2	4	4	3	0
Section 3	4	4	3	0

TABLE II: A summary of numbers of available traces in the data set.

	$800\ MHz$		$1.2\ GHz$	
Antenna height	$20\ cm$	$30\ cm$	$20\ cm$	$30\ cm$
Section 1	333	334	249	249
Section 2	340	340	255	0
Section 3	308	310	232	0
Total	981	984	736	249

C. Feature extraction example

Three traces from sections of different ballast are shown in Fig. 6. There are 308 samples in each trace. In terms of the waveforms, the traces are analogous to each other for a human operator, and it is hard to distinguish them. However, the discrete Fourier transform of these traces significantly improves the visualisation of the variance (see Fig. 7), and thus it is possible to extract features to classify the traces.

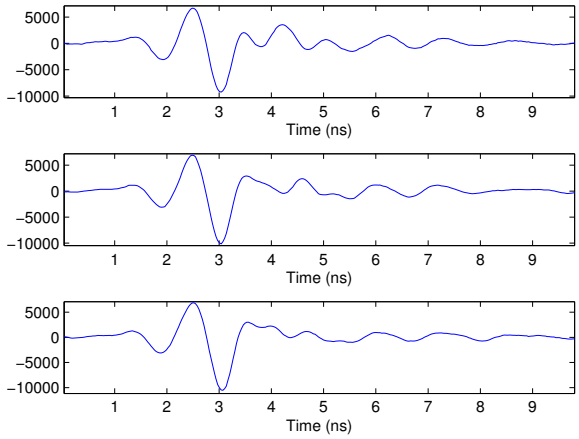

Fig. 6: Three traces of railway data set from ballast with 50% clay, clean ballast and ballast with 50% coal, respectively.

Though the discrete Fourier transform can be used as an input of the classification system, it may introduce computational complexity. In the proposed system, two techniques are employed to solve this issue. The first technique is normalisation; it is applied on each feature vector to ensure the consistency of magnitude spectrum amplitudes. The second technique is automatic feature selection. Magnitude spectrum amplitude features are extracted at automatically selected points and fed into classification components.

An example of feature points are shown in Fig. 8. Each vertical dotted line indicates a frequency where an amplitude feature is extracted. There are 17 feature points in this example which mean each trace is represented by a feature vector of size 17. Compared to the length of the discrete Fourier

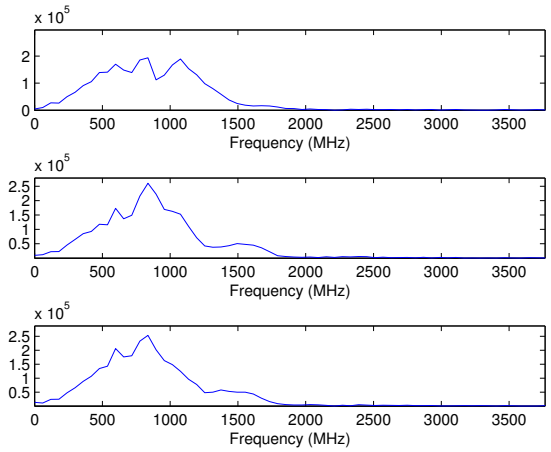

Fig. 7: Magnitude spectra of the three traces shown in Fig. 6.

transform that is greater than 308, the automatic feature selection strategy considerably reduces the feature size.

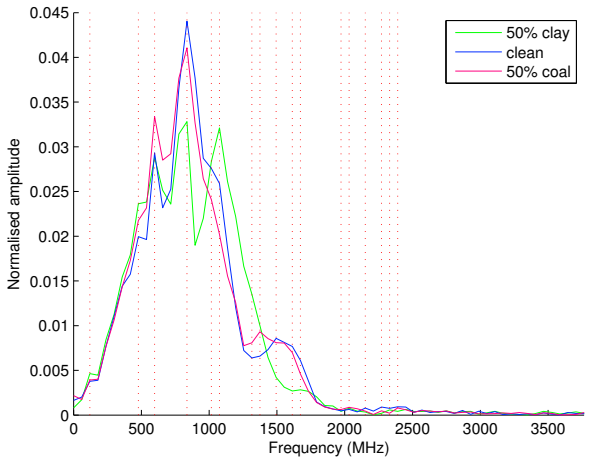

Fig. 8: Feature points of the three traces shown in Fig. 6. Each vertical dotted line represents a feature point.

D. Experimental results

In the experiments, we train the system using a portion of the 800 MHz data with an antenna height of 20 cm. Then the system is tested using the remaining data with the same antenna frequency and antenna height. Because in our system the traces are shifted according to the global maximum points, we are interested in the system performance when the GPR signals are obtained with a different set-up of antenna height. Therefore, the trained system is tested using data at 30 cm antenna height with the same antenna frequency. We also train the system with 30 cm data and test it with both 20 cm and 30 cm data.

We use five-fold cross validation to search for the optimal parameters of support vector machines. An issue arises here is that five-fold cross validation sometimes finds more than one set of optimum parameters. To solve this problem, we simply construct a number of pair-wise SVM classifiers using the chosen parameters and form them as a pair-wise SVMs pool. Whenever a test set is input to the system, it will be evaluated by every pair-wise SVMs classifier in the pool.

The system performance is measured by averaging the classification rates of all pair-wise SVMs. Note that during each test, the training set is randomly split from the whole data set. The comprehensive experimental results are given in Tables III and IV. Figure 9 also shows the experimental results when the system is trained with data of 20 cm antenna height.

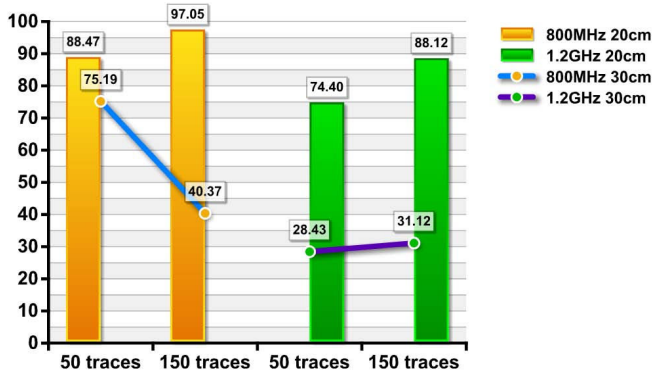

Fig. 9: Classification rates of the system on the test sets; the system is trained with data of 20 cm antenna height. The bars represent the classification rates on 20 cm test data sets, and the lines show the classification rates on 30 cm test data sets.

Using 800 MHz data of 20 cm antenna height to train the system, when we increase the training data set from 50 to 150 traces, there is a significant increase in the average classification rate, from 88.47% to 97.05% (see Fig. 9). When the trained system is tested on the 30 cm data, the average classification rate drops to 40.37%. However, the classification rate of 74.57% with 50 trace-trained system on the 30 cm data can be considered as an anomaly. If we use 30 cm data to train the system, the average classification rate on the 30 cm test set increase slightly from 94.52% to 97.05%; and the classification rates on the 20 cm test set are 52.08% and 55.95%.

Based on the results, when the training set size is increased from 50 to 150, the classification rate on the test set with the same antenna height is improved. However, the system performs poorly when the data of a different antenna height is tested. A possible explanation is that due to spherical wave propagation, the data of different antenna heights contain different interference from underground. Moreover, the GPR signal attenuation affects significantly the reflected waves.

V. Conclusion

In this paper, we have presented an automatic classification system for ground penetrating radar signals. The system is based on magnitude spectrum amplitude features and support vector machines. The feature extraction and classification

TABLE III: Classification rates of the system on the test sets; the system is trained with data of 20 cm antenna height.

Antenna frequency	Training data	Average classification rate /test set size	
		20 cm data	30 cm data
800 MHz	50 traces 20 cm antenna height	88.47% 774	75.19% 924
	150 traces 20 cm antenna height	97.05% 474	40.37% 924
1.2 GHz	50 traces 20 cm antenna height	74.40% 546	28.43% 232
	150 traces 20 cm antenna height	88.12% 450	31.12% 232

TABLE IV: Classification rates of the system on the test sets; the system is trained with data of 30 cm antenna height.

Antenna frequency	Training data	Average classification rate /test set size	
		20 cm data	30 cm data
800 MHz	50 traces 30 cm antenna height	52.08% 924	94.52% 774
	150 traces 30 cm antenna height	55.95% 924	97.05% 474

stages are operated automatically. The experimental results have verified that the system performs well in ballast classification with a classification rate reaching 97%. In future research, we aim to investigate time-frequency features and improve the system performance in terms of antenna height.

ACKNOWLEDGMENT

The railway data is provided by the 'CRC Rail for Innovation' as part of Rail CRC-AT5 project.

REFERENCES

[1] A. P. Annan, "GPR - history, trends, and future developments," *Subsurface Sensing Technologies and Applications*, vol. 3, no. 4, pp. 253–270, 2002.

[2] D. J. Daniels, Ed., *Ground Penetrating Radar*, 2nd ed. London: The Institution of Electrical Engineers, 2004.

[3] A. Neal, "Ground-penetrating radar and its use in sedimentology: principles, problems and progress," *Earth-Science Reviews*, vol. 66, no. 3-4, pp. 261–330, 2004.

[4] H. M. Jol, Ed., *Ground Penetrating Radar Theory and Applications*, 1st ed. Amsterdam: Elsevier Science, 2009.

[5] A. P. Annan, "Practical processing of GPR data," in *Proceedings of the Second Government Workshop on Ground Penetrating Radar*, Columbus, Ohio, 1993.

[6] C. Hauck and C. Kneisel, Eds., *Applied Geophysics in Periglacial Environments. [electronic resource]*. Leiden: Cambridge University Press, 2008.

[7] P. Xavier Neto and W. Eugłnio de Medeiros, "A practical approach to correct attenuation effects in GPR data," *Journal of Applied Geophysics*, vol. 59, no. 2, pp. 140–151, 2006.

[8] J. M. Reynolds, *An Introduction to Applied and Environmental Geophysics*. New York: John Wiley, 1996.

[9] A. Papandreou-Suppappola, Ed., *Applications in time-frequency signal processing*, ser. Electrical engineering and applied signal processing series. London: CRC Press LLC, 2003.

[10] V. C. Chen and H. Ling, *Time-Frequency Transforms for Radar Imaging and Signal Analysis*. Boston: Artech House, 2002.

[11] I. L. Al-Qadi, W. Xie, and R. Roberts, "Time-frequency approach for ground penetrating radar data analysis to assess railroad ballast condition," *Research in Nondestructive Evaluation*, vol. 19, no. 4, pp. 219 – 237, 2008.

[12] S. Shihab, O. Zahran, and W. Al-Nuaimy, "Time-frequency characteristics of ground penetrating radar reflections from railway ballast and plant," in *7th IEEE High Frequency Postgraduate Student Colloquium*, 2002.

[13] S. Sinha, P. S. Routh, P. D. Anno, and J. P. Castagna, "Spectral decomposition of seismic data with continuous-wavelet transform," *Geophysics*, vol. 70, no. 6, pp. 19–25, 2005.

[14] M. Fujimoto, K. Nonami, A. Tatsuo, Y. Shigeru, and M. Kazuhisa, "Mine detection algorithm using pattern classification method by sensor fusion–experimental results by means of GPR," in *Systems and Human Science*. Amsterdam: Elsevier Science, 2005, pp. 259–274.

[15] S. Abe, *Support Vector Machines for Pattern Classification*. New York: Springer, 2005.

[16] A. Moore, *Statistical data mining tutorials: support vector machines*, 2001. [Online]. Available: http://www.autonlab.org/tutorials/

[17] B. Moghaddam and M.-H. Yang, "Learning gender with support faces," *IEEE Transactions on Pattern Analysis and Machine Intelligence*, vol. 24, no. 5, pp. 707–711, 2002.

[18] C.-C. Chang and C.-J. Lin, *LIBSVM: a library for support vector machines*, 2007. [Online]. Available: http://www.csie.ntu.edu.tw/ cjlin/libsvm/